

Achievable Rates and Resource Allocation Strategies for Imperfectly-Known Fading Relay Channels

Junwei Zhang and Mustafa Cenk Gursoy

Abstract

In this paper, achievable rates and resource allocation strategies for imperfectly-known fading relay channels are studied. It is assumed that communication starts with the network training phase in which the receivers estimate the fading coefficients of the channels. In the data transmission phase, amplify-and-forward and decode-and-forward relaying schemes with different degrees of cooperation are considered, and the corresponding achievable rate expressions are obtained. Three resource allocation problems are addressed: 1) power allocation between data and training symbols; 2) time/bandwidth allocation to the relay; 3) power allocation between the source and relay in the presence of total power constraints. The achievable rate expressions are employed to identify efficient resource allocation strategies. Several observations with important practical implications are made. It is noted that unless the source-relay channel quality is high, cooperation is not beneficial and noncooperative direct transmission should be preferred at high signal-to-noise ratio (SNR) values when amplify-and-forward or decode-and-forward with repetition coding is employed as the cooperation strategy. On the other hand, relaying is shown to generally improve the performance at low SNRs. Additionally, transmission schemes in which the relay and source transmit in non-overlapping intervals are seen to perform better in the low-SNR regime. Finally, through a bit energy analysis, it is noted that care should be exercised when operating at very low SNR levels, as energy efficiency significantly degrades below a certain SNR threshold value.

Index Terms: Achievable rates, amplify-and-forward relaying, channel estimation, cooperative transmission, decode-and-forward relaying, energy efficiency in the low-power regime, imperfectly-known fading channels, resource allocation schemes, relay channel, training.

Junwei Zhang and Mustafa Cenk Gursoy are with the Department of Electrical Engineering, University of Nebraska-Lincoln, Lincoln, NE, 68588 (e-mail: junwei.zhang@huskers.unl.edu, gursoy@engr.unl.edu).

This work was supported in part by the NSF CAREER Grant CCF-0546384. The material in this paper was presented in part at the 45th Annual Allerton Conference on Communication, Control and Computing in Sept. 2007, and in part at the 9th IEEE Workshop on Signal Processing Advances for Wireless Communications (SPAWC) in July 2008.

I. INTRODUCTION

In wireless communications, deterioration in performance is experienced due to various impediments such as interference, fluctuations in power due to reflections and attenuation, and randomly-varying channel conditions caused by mobility and changing environment. Recently, cooperative wireless communications has attracted much interest as a technique that can mitigate these degradations and provide higher rates or improve the reliability through diversity gains. The relay channel was first introduced by van der Meulen in [1], and initial research was primarily conducted to understand the rates achieved in relay channels [2], [3]. More recently, diversity gains of cooperative transmission techniques have been studied in [4]–[7]. In [6], several cooperative protocols have been proposed, with amplify-and-forward (AF) and decode-and-forward (DF) being the two basic relaying schemes. The performance of these protocols are characterized in terms of outage events and outage probabilities. In [8], three different time-division AF and DF cooperative protocols with different degrees of broadcasting and receive collision are studied. Resource allocation for relay channel and networks has been addressed in several studies (see e.g., [9]–[14]). In [9], upper and lower bounds on the outage and ergodic capacities of relay channels are obtained under the assumption that the channel side information (CSI) is available at both the transmitter and receiver. Power allocation strategies are explored in the presence of a total power constraint on the source and relay. In [10], under again the assumption of the availability of CSI at the receiver and transmitter, optimal dynamic resource allocation methods in relay channels are identified under total average power constraints and delay limitations by considering delay-limited capacities and outage probabilities as performance metrics. In [11], resource allocation schemes in relay channels are studied in the low-power regime when only the receiver has perfect CSI. Liang *et al.* in [12] investigated resource allocation strategies under separate power constraints at the source and relay nodes, and showed that the optimal strategies differ depending on the channel statics and the values of the power constraints. Recently, the impact of channel state information (CSI) and power allocation on rates of transmission over fading relay channels are studied in [14] by Ng and Goldsmith. The authors analyzed the cases of full CSI and receiver only CSI, considered the optimum or equal power allocation between the source and relay nodes, and identified the best strategies in different cases. In general, the area has seen an explosive growth in the number of studies (see additionally e.g., [15] – [17], and references therein). An excellent review of cooperative strategies from both rate and diversity improvement perspectives is provided in [18] in which the impacts of cooperative schemes on

device architecture and higher-layer wireless networking protocols are also addressed. Recently, a special issue has been dedicated to models, theory, and codes for relaying and cooperation in communication networks in [19].

As noted above, studies on relaying and cooperation are numerous. However, most work has assumed that the channel conditions are perfectly known at the receiver and/or transmitter sides. Especially in mobile applications, this assumption is unwarranted as randomly-varying channel conditions can be learned by the receivers only imperfectly. Moreover, the performance analysis of cooperative schemes in such scenarios is especially interesting and called for because relaying introduces additional channels and hence increases the uncertainty in the model if the channels are known only imperfectly. Recently, Wang *et al.* in [20] considered pilot-assisted transmission over wireless sensory relay networks, and analyzed scaling laws achieved by the amplify-and-forward scheme in the asymptotic regimes of large nodes, large block length, and small signal-to-noise ratio (SNR) values. In this study, the channel conditions are being learned only by the relay nodes. In [21] and [22], estimation of the overall source-relay-destination channel is addressed for amplify-and-forward relay channels. In [21], Gao *et al.* considered both the least squares (LS) and minimum-mean-square error (MMSE) estimators, and provided optimization formulations and guidelines for the design of training sequences and linear precoding matrices. In [22], under the assumption of fixed power allocation between data transmission and training, Patel and Stüber analyzed the performance of linear MMSE estimation in relay channels. In both [21] and [22], the training design is studied in an estimation-theoretic framework, and mean-square errors and bit error rates, rather than the achievable rates, are considered as performance metrics. To the best of our knowledge, performance analysis and resource allocation strategies have still not been sufficiently addressed for imperfectly-known relay channels in an information-theoretic context by considering rate expressions. We note that Avestimehr and Tse in [23] studied the outage capacity of slow fading relay channels. They showed that Bursty Amplify-Forward strategy achieves the outage capacity in the low SNR and low outage probability regime. Interestingly, they further proved that the optimality of Bursty AF is preserved even if the receivers do not have prior knowledge of the channels.

In this paper, we study the imperfectly-known fading relay channels. We assume that transmission takes place in two phases: *network training phase* and *data transmission phase*. In the network training phase, a-priori unknown fading coefficients are estimated at the receivers with the assistance of pilot symbols. Following the training phase, AF and DF relaying techniques are employed in the data transmission. Our contributions in this paper are the

following:

- 1) We obtain achievable rate expressions for AF and DF relaying protocols with different degrees of cooperation, ranging from noncooperative communications to full cooperation. We provide a unified analysis that applies to both overlapped and non-overlapped transmissions of the source and relay. We note that achievable rates are obtained by considering the ergodic scenario in which the transmitted codewords are assumed to be sufficiently long to span many fading realizations.
- 2) We identify resource allocation strategies that maximize the achievable rates. We consider three types of resource allocation problems:
 - a) power allocation between data and training symbols;
 - b) time/bandwidth allocation to the relay;
 - c) power allocation between the source and relay if there is a total power constraint in the system.
- 3) We investigate the energy efficiency in imperfectly-known relay channels by finding the bit energy requirements in the low-SNR regime.

The organization of the rest of the paper is as follows. In Section II, we describe the channel model. Network training and data transmission phases are explained in Section III. We obtain the achievable rate expressions in Section IV and study the resource allocation strategies in Section V. We discuss the energy efficiency in the low-SNR regime in Section VI. Finally, we provide conclusions in Section VII. The proofs of the achievable rate expressions are relegated to the Appendix.

II. CHANNEL MODEL

We consider a three-node relay network which consists of a source, destination, and a relay node. This relay network model is depicted in Figure 1. Source-destination, source-relay, and relay-destination channels are modeled as Rayleigh block-fading channels with fading coefficients denoted by h_{sd} , h_{sr} , and h_{rd} , respectively for each channel. Due to the block-fading assumption, the fading coefficients $h_{sr} \sim \mathcal{CN}(0, \sigma_{sr}^2)$, $h_{sd} \sim \mathcal{CN}(0, \sigma_{sd}^2)$, and $h_{rd} \sim \mathcal{CN}(0, \sigma_{rd}^2)$ stay constant for a block of m symbols before they assume independent realizations for the following block¹. In this system, the source node tries to send information to the destination node with the help of

¹ $x \sim \mathcal{CN}(d, \sigma^2)$ is used to denote a proper complex Gaussian random variable with mean d and variance σ^2 .

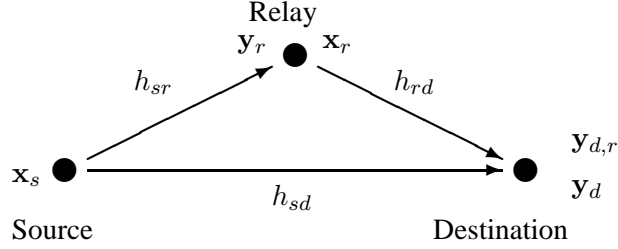


Fig. 1. Three-node relay network model

the intermediate relay node. It is assumed that the source, relay, and destination nodes do not have prior knowledge of the realizations of the fading coefficients. The transmission is conducted in two phases: *network training phase* in which the fading coefficients are estimated at the receivers, and *data transmission phase*. Overall, the source and relay are subject to the following power constraints in one block:

$$|x_{s,t}|^2 + E\{\|\mathbf{x}_s\|^2\} \leq mP_s, \quad (1)$$

$$|x_{r,t}|^2 + E\{\|\mathbf{x}_r\|^2\} \leq mP_r, \quad (2)$$

where $x_{s,t}$ and $x_{r,t}$ are the training symbols sent by the source and relay, respectively, and \mathbf{x}_s and \mathbf{x}_r are the corresponding source and relay data vectors. The pilot symbols enable the receivers to obtain the minimum mean-square error (MMSE) estimates of the fading coefficients. Since MMSE estimates depend only on the total training power but not on the training duration, transmission of a single pilot symbol is optimal for average-power limited channels. The transmission structure in each block is shown in Fig. 2. As observed immediately, the first two symbols are dedicated to training while data transmission occurs in the remaining duration of $m - 2$ symbols. Detailed description of the network training and data transmission phases is provided in the following section.

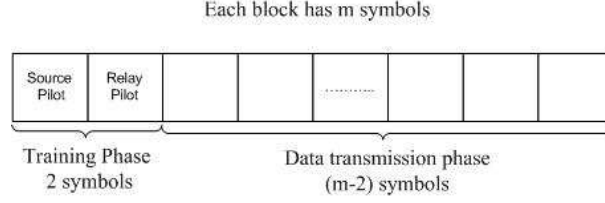


Fig. 2. Transmission structure in a block of m symbols.

III. NETWORK TRAINING AND DATA TRANSMISSION

A. Network Training Phase

Each block transmission starts with the training phase. In the first symbol period, source transmits the pilot symbol $x_{s,t}$ to enable the relay and destination to estimate the channel coefficients h_{sr} and h_{sd} , respectively. The signals received by the relay and destination are

$$y_{r,t} = h_{sr}x_{s,t} + n_r, \quad \text{and} \quad y_{d,t} = h_{sd}x_{s,t} + n_d, \quad (3)$$

respectively. Similarly, in the second symbol period, relay transmits the pilot symbol $x_{r,t}$ to enable the destination to estimate the channel coefficient h_{rd} . The signal received by the destination is

$$y_{d,r,t} = h_{rd}x_{r,t} + n_{d,r}. \quad (4)$$

In the above formulations, $n_r \sim \mathcal{CN}(0, N_0)$, $n_d \sim \mathcal{CN}(0, N_0)$, and $n_{d,r} \sim \mathcal{CN}(0, N_0)$ represent independent Gaussian random variables. Note that n_d and $n_{d,r}$ are Gaussian noise samples at the destination in different time intervals, while n_r is the Gaussian noise at the relay.

In the training process, it is assumed that the receivers employ minimum mean-square-error (MMSE) estimation. We assume that the source allocates δ_s fraction of its total power mP_s for training while the relay allocates δ_r fraction of its total power mP_r for training. As described in [31], the MMSE estimate of h_{sr} is given by

$$\hat{h}_{sr} = \frac{\sigma_{sr}^2 \sqrt{\delta_s m P_s}}{\sigma_{sr}^2 \delta_s m P_s + N_0} y_{r,t}, \quad (5)$$

where $y_{r,t} \sim \mathcal{CN}(0, \sigma_{sr}^2 \delta_s m P_s + N_0)$. We denote by \tilde{h}_{sr} the estimate error which is a zero-mean complex Gaussian random variable with variance $\text{var}(\tilde{h}_{sr}) = \frac{\sigma_{sr}^2 N_0}{\sigma_{sr}^2 \delta_s m P_s + N_0}$. Similarly, for the fading coefficients h_{sd} and h_{rd} , we have the following estimates and estimate error variances:

$$\hat{h}_{sd} = \frac{\sigma_{sd}^2 \sqrt{\delta_s m P_s}}{\sigma_{sd}^2 \delta_s m P_s + N_0} y_{d,t}, \quad y_{d,t} \sim \mathcal{CN}(0, \sigma_{sd}^2 \delta_s m P_s + N_0), \quad \text{var}(\tilde{h}_{sd}) = \frac{\sigma_{sd}^2 N_0}{\sigma_{sd}^2 \delta_s m P_s + N_0}, \quad (6)$$

$$\hat{h}_{rd} = \frac{\sigma_{rd}^2 \sqrt{\delta_r m P_r}}{\sigma_{rd}^2 \delta_r m P_r + N_0} y_{d,r,t}, \quad y_{d,r,t} \sim \mathcal{CN}(0, \sigma_{rd}^2 \delta_r m P_r + N_0), \quad \text{var}(\tilde{h}_{rd}) = \frac{\sigma_{rd}^2 N_0}{\sigma_{rd}^2 \delta_r m P_r + N_0}. \quad (7)$$

With these estimates, the fading coefficients can now be expressed as

$$h_{sr} = \hat{h}_{sr} + \tilde{h}_{sr}, \quad h_{sd} = \hat{h}_{sd} + \tilde{h}_{sd}, \quad h_{rd} = \hat{h}_{rd} + \tilde{h}_{rd}. \quad (8)$$

B. Data Transmission Phase

As discussed in the previous section, within a block of m symbols, the first two symbols are allocated to network training. In the remaining duration of $m - 2$ symbols, data transmission takes place. Throughout the paper, we consider several transmission protocols which can be classified into two categories depending on whether or not the source and relay simultaneously transmit information: *non-overlapped* and *overlapped transmissions*. Since the practical relay node usually cannot transmit and receive data simultaneously, we assume that the relay works under half-duplex constraint. Hence, the relay first listens and then transmits. We introduce the relay transmission parameter α and assume that $\alpha(m - 2)$ symbols are allocated for relay transmission. Hence, α can be seen as the fraction of total time or bandwidth allocated to the relay. Note that the parameter α enables us to control the degree of cooperation. In non-overlapped transmission protocol, source and relay transmit over non-overlapping intervals. Therefore, source transmits over a duration of $(1 - \alpha)(m - 2)$ symbols and becomes silent as the relay transmits. On the other hand, in overlapped transmission protocol, source transmits all the time and sends $m - 2$ symbols in each block.

We assume that the source transmits at a per-symbol power level of P_{s1} when the relay is silent, and P_{s2} when the relay is in transmission. Clearly, in non-overlapped mode, $P_{s2} = 0$. On the other hand, in overlapped transmission, we assume $P_{s1} = P_{s2}$. Noting that the total power available after the transmission of the pilot symbol

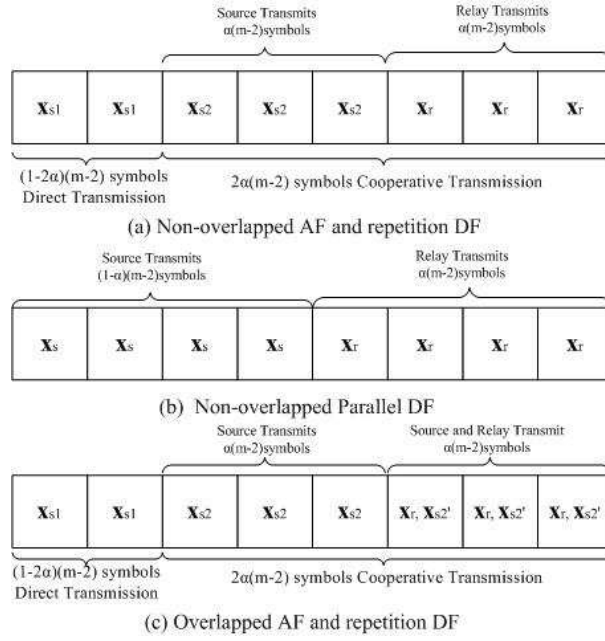


Fig. 3. Transmission structure and order in the data transmission phase for different cooperation schemes.

is $(1 - \delta_s)mP_s$, we can write

$$(1 - \alpha)(m - 2)P_{s1} + \alpha(m - 2)P_{s2} = (1 - \delta_s)mP_s. \quad (9)$$

The above assumptions imply that power for data transmission is equally distributed over the symbols during the transmission periods. Hence, in non-overlapped and overlapped modes, the symbol powers are $P_{s1} = \frac{(1-\delta_s)mP_s}{(1-\alpha)(m-2)}$ and $P_{s1} = P_{s2} = \frac{(1-\delta_s)mP_s}{(m-2)}$, respectively. Furthermore, we assume that the power of each symbol transmitted by the relay node is P_{r1} , which satisfies, similarly as above,

$$\alpha(m - 2)P_{r1} = (1 - \delta_r)mP_r. \quad (10)$$

Next, we provide detailed descriptions of non-overlapped and overlapped cooperative transmission schemes.

1) Non-overlapped transmission: We first consider the two simplest cooperative protocols: *non-overlapped AF* where the relay amplifies the received signal and forwards it to the destination, and *non-overlapped DF with repetition coding* where the relay decodes the message, re-encodes it using the same codebook as the source, and

forwards it. In these protocols, since the relay either amplifies the received signal, or decodes it but uses the same codebook as the source when forwarding, source and relay should be allocated equal time slots in the cooperation phase. Therefore, before cooperation starts, we initially have direct transmission from the source to the destination without any aid from the relay over a duration of $(1 - 2\alpha)(m - 2)$ symbols. In this phase, source sends the $(1 - 2\alpha)(m - 2)$ -dimensional data vector \mathbf{x}_{s1} and the received signal at the destination is given by

$$\mathbf{y}_{d1} = h_{sd}\mathbf{x}_{s1} + \mathbf{n}_{d1}. \quad (11)$$

Subsequently, cooperative transmission starts. At first, the source transmits the $\alpha(m - 2)$ -dimensional data vector \mathbf{x}_{s2} which is received at the the relay and the destination, respectively, as

$$\mathbf{y}_r = h_{sr}\mathbf{x}_{s2} + \mathbf{n}_r, \quad \text{and} \quad \mathbf{y}_{d2} = h_{sd}\mathbf{x}_{s2} + \mathbf{n}_{d2}. \quad (12)$$

In (11) and (12), \mathbf{n}_{d1} and \mathbf{n}_{d2} are independent Gaussian noise vectors composed of independent and identically distributed (i.i.d.), circularly symmetric, zero-mean complex Gaussian random variables with variance N_0 , modeling the additive background noise at the transmitter in different transmission phases. Similarly, \mathbf{n}_r is a Gaussian noise vector at the relay, whose components are i.i.d. zero-mean Gaussian random variables with variance N_0 . For compact representation, we denote the overall source data vector by $\mathbf{x}_s = [\mathbf{x}_{s1}^T \ \mathbf{x}_{s2}^T]^T$, and the signal received at the destination directly from the source by $\mathbf{y}_d = [\mathbf{y}_{d1}^T \ \mathbf{y}_{d2}^T]^T$ where T denotes the transpose operation. After completing its transmission, the source becomes silent, and the relay transmits an $\alpha(m - 2)$ -dimensional symbol vector \mathbf{x}_r which is generated from the previously received \mathbf{y}_r [6] [7]. Now, the destination receives

$$\mathbf{y}_{d,r} = h_{rd}\mathbf{x}_r + \mathbf{n}_{d,r}. \quad (13)$$

After substituting the estimate expressions in (8) into (11)–(13), we have

$$\mathbf{y}_{d1} = \hat{h}_{sd}\mathbf{x}_{s1} + \tilde{h}_{sd}\mathbf{x}_{s1} + \mathbf{n}_{d1}, \quad \mathbf{y}_r = \hat{h}_{sr}\mathbf{x}_{s2} + \tilde{h}_{sr}\mathbf{x}_{s2} + \mathbf{n}_r, \quad \mathbf{y}_{d2} = \hat{h}_{sd}\mathbf{x}_{s2} + \tilde{h}_{sd}\mathbf{x}_{s2} + \mathbf{n}_{d2}, \quad (14)$$

$$\mathbf{y}_{d,r} = \hat{h}_{rd}\mathbf{x}_r + \tilde{h}_{rd}\mathbf{x}_r + \mathbf{n}_{d,r}. \quad (15)$$

Note that we have $0 < \alpha \leq 1/2$ for AF and repetition coding DF. Therefore, $\alpha = 1/2$ models full cooperation while we have noncooperative communications as $\alpha \rightarrow 0$. It should also be noted that α should in general be

chosen such that $\alpha(m - 2)$ is an integer. The transmission structure and order in the data transmission phase of non-overlapped AF and repetition DF are depicted Fig. 3.a, together with the notation used for the data symbols sent by the source and relay.

For non-overlapped transmission, we also consider *DF with parallel channel coding*, in which the relay uses a different codebook to encode the message. In this case, the source and relay do not have to be allocated the same duration in the cooperation phase. Therefore, source transmits over a duration of $(1 - \alpha)(m - 2)$ symbols while the relay transmits in the remaining duration of $\alpha(m - 2)$ symbols. Clearly, the range of α is now $0 < \alpha < 1$. In this case, the input-output relations are given by (12) and (13). Since there is no separate direct transmission, $\mathbf{x}_{s2} = \mathbf{x}_s$ and $\mathbf{y}_{d2} = \mathbf{y}_d$ in (12). Moreover, the dimensions of the vectors $\mathbf{x}_s, \mathbf{y}_d, \mathbf{y}_r$ are now $(1 - \alpha)(m - 2)$, while \mathbf{x}_r and $\mathbf{y}_{d,r}$ are vectors of dimension $\alpha(m - 2)$. Fig. 3.b provides a graphical description of the transmission order for non-overlapped parallel DF scheme.

2) Overlapped transmission: In this category, we consider a more general and complicated scenario in which the source transmits all the time. We study AF and repetition DF, in which we, similarly as in the non-overlapped model, have unaided direct transmission from the source to the destination in the initial duration of $(1 - 2\alpha)(m - 2)$ symbols. Cooperative transmission takes place in the remaining duration of $2\alpha(m - 2)$ symbols. Again, we have $0 < \alpha \leq 1/2$ in this setting. In these protocols, the input-output relations are expressed as follows:

$$\mathbf{y}_{d1} = h_{sd}\mathbf{x}_{s1} + \mathbf{n}_{d1}, \quad \mathbf{y}_r = h_{sr}\mathbf{x}_{s2} + \mathbf{n}_r, \quad \mathbf{y}_{d2} = h_{sd}\mathbf{x}_{s2} + \mathbf{n}_{d2}, \quad \text{and} \quad \mathbf{y}_{d,r} = h_{sd}\mathbf{x}'_{s2} + h_{rd}\mathbf{x}_r + \mathbf{n}_{d,r}. \quad (16)$$

Above, $\mathbf{x}_{s1}, \mathbf{x}_{s2}, \mathbf{x}'_{s2}$, which have respective dimensions of $(1 - 2\alpha)(m - 2), \alpha(m - 2)$ and $\alpha(m - 2)$, represent the source data vectors sent in direct transmission, cooperative transmission when relay is listening, and cooperative transmission when relay is transmitting, respectively. Note again that the source transmits all the time. \mathbf{x}_r is the relay's data vector with dimension $\alpha(m - 2)$. $\mathbf{y}_{d1}, \mathbf{y}_{d2}, \mathbf{y}_{d,r}$ are the corresponding received vectors at the destination, and \mathbf{y}_r is the received vector at the relay. The input vector \mathbf{x}_s now is defined as $\mathbf{x}_s = [\mathbf{x}_{s1}^T, \mathbf{x}_{s2}^T, \mathbf{x}'_{s2}{}^T]^T$ and we again denote $\mathbf{y}_d = [\mathbf{y}_{d1}^T, \mathbf{y}_{d2}^T]^T$. If we express the fading coefficients as $h = \hat{h} + \tilde{h}$ in (16), we obtain the following

input-output relations:

$$\mathbf{y}_{d1} = \hat{h}_{sd}\mathbf{x}_{s1} + \tilde{h}_{sd}\mathbf{x}_{s1} + \mathbf{n}_{d1}, \quad \mathbf{y}_r = \hat{h}_{sr}\mathbf{x}_{s2} + \tilde{h}_{sr}\mathbf{x}_{s2} + \mathbf{n}_r, \quad \mathbf{y}_{d2} = \hat{h}_{sd}\mathbf{x}_{s2} + \tilde{h}_{sd}\mathbf{x}_{s2} + \mathbf{n}_{d2}, \quad \text{and} \quad (17)$$

$$\mathbf{y}_{d,r} = \hat{h}_{sd}\mathbf{x}'_{s2} + \hat{h}_{rd}\mathbf{x}_r + \tilde{h}_{sd}\mathbf{x}'_{s2} + \tilde{h}_{rd}\mathbf{x}_r + \mathbf{n}_{d,r}. \quad (18)$$

A graphical depiction of the transmission order for overlapped AF and repetition DF is given in Fig. 3.c.

Finally, the list of notations used throughout the paper is given in Table I.

IV. ACHIEVABLE RATES

In this section, we provide achievable rate expressions for AF and DF relaying in both non-overlapped and overlapped transmission scenarios in a unified fashion. Achievable rate expressions are obtained by considering the estimate errors as additional sources of Gaussian noise. Since Gaussian noise is the worst uncorrelated additive noise for a Gaussian model [26, Appendix], [27], achievable rates given in this section can be regarded as worst-case rates.

We first consider AF relaying scheme. The capacity of the AF relay channel is the maximum mutual information between the transmitted signal \mathbf{x}_s and received signals \mathbf{y}_d and $\mathbf{y}_{d,r}$ given the estimates $\hat{h}_{sr}, \hat{h}_{sd}, \hat{h}_{rd}$:

$$C_{AF} = \sup_{p_{\mathbf{x}_s}(\cdot)} \frac{1}{m} I(\mathbf{x}_s; \mathbf{y}_d, \mathbf{y}_{d,r} | \hat{h}_{sr}, \hat{h}_{sd}, \hat{h}_{rd}). \quad (19)$$

Note that this formulation presupposes that the destination has the knowledge of \hat{h}_{sr} . Hence, we assume that the value of \hat{h}_{sr} is forwarded reliably from the relay to the destination over low-rate control links. In general, solving the optimization problem in (19) and obtaining the AF capacity is a difficult task. Therefore, we concentrate on finding a lower bound on the capacity. A lower bound is obtained by replacing the product of the estimate error and the transmitted signal in the input-output relations with the worst-case noise with the same correlation. Therefore, we consider in the overlapped AF scheme

$$\mathbf{z}_{d1} = \tilde{h}_{sd}\mathbf{x}_{s1} + \mathbf{n}_{d1}, \quad \mathbf{z}_r = \tilde{h}_{sr}\mathbf{x}_{s2} + \mathbf{n}_r, \quad \mathbf{z}_{d2} = \tilde{h}_{sd}\mathbf{x}_{s2} + \mathbf{n}_{d2}, \quad \mathbf{z}_{d,r} = \tilde{h}_{sd}\mathbf{x}'_{s2} + \tilde{h}_{rd}\mathbf{x}_r + \mathbf{n}_{d,r}, \quad (20)$$

as noise vectors with covariance matrices

$$E\{\mathbf{z}_{d1}\mathbf{z}_{d1}^\dagger\} = \sigma_{z_{d1}}^2 \mathbf{I} = \sigma_{\tilde{h}_{sd}}^2 E\{\mathbf{x}_{s1}\mathbf{x}_{s1}^\dagger\} + N_0\mathbf{I}, \quad E\{\mathbf{z}_r\mathbf{z}_r^\dagger\} = \sigma_{z_r}^2 \mathbf{I} = \sigma_{\tilde{h}_{sr}}^2 E\{\mathbf{x}_{s2}\mathbf{x}_{s2}^\dagger\} + N_0\mathbf{I}, \quad (21)$$

TABLE I
LIST OF NOTATIONS

h_{sd}	source-destination channel fading coefficient
h_{sr}	relay-destination channel fading coefficient
h_{rd}	relay-destination channel fading coefficient
\hat{h}	estimate of the fading coefficient h .
\tilde{h}	error in the estimate of the fading coefficient h .
σ^2	variance of random variables
N_0	variance of Gaussian random variables due to thermal noise
m	number of symbols in each block
mP_s	total average power of the source in each block of m symbols
mP_r	total average power of the relay in each block of m symbols
δ_s	fraction of total power allocated to training by the source
δ_r	fraction of total power allocated to training by the relay
$x_{s,t}$	pilot symbol sent by the source
$x_{r,t}$	pilot symbol sent by the relay
n_d	additive Gaussian noise at the destination in the interval in which the source pilot symbol is sent
n_r	additive Gaussian noise at the relay in the interval in which the source pilot symbol is sent
$n_{d,r}$	additive Gaussian noise at the destination in the interval in which the relay pilot symbol is sent
$y_{d,t}$	received signal at the destination in the interval in which the source pilot symbol is sent
$y_{r,t}$	received signal at the relay in the interval in which the source pilot symbol is sent
$y_{d,r,t}$	received signal at the destination in the interval in which the relay pilot symbol is sent
P_{s1}	power of each source symbol sent in the interval in which the relay is not transmitting
P_{s2}	power of each source symbol sent in the interval in which the relay is transmitting
P_{r1}	power of each relay symbol
α	fraction of time/bandwidth allocated to the relay
\mathbf{x}_{s1}	$(1 - 2\alpha)(m - 2)$ -dimensional data vector sent by the source in the noncooperative transmission mode
\mathbf{x}_{s2}	data vector sent by the source when the relay is listening. The dimension is $\alpha(m - 2)$ for AF and repetition DF, and $(1 - \alpha)(m - 2)$ for parallel DF
\mathbf{x}'_{s2}	$\alpha(m - 2)$ -dimensional data vector sent by the source when the relay is transmitting
\mathbf{x}_r	$\alpha(m - 2)$ -dimensional data vector sent by the relay
\mathbf{n}_{d1}	$(1 - 2\alpha)(m - 2)$ -dimensional noise vector at the destination in the noncooperative transmission mode
\mathbf{n}_{d2}	noise vector at the destination in the interval when the relay is listening. The dimension is $\alpha(m - 2)$ for AF and repetition DF, and $(1 - \alpha)(m - 2)$ for parallel DF
$\mathbf{n}_{d,r}$	$\alpha(m - 2)$ -dimensional noise vector at the destination in the interval when the relay is transmitting
\mathbf{n}_r	noise vector at the relay. The dimension is $\alpha(m - 2)$ for AF and repetition DF, and $(1 - \alpha)(m - 2)$ for parallel DF
\mathbf{y}_{d1}	$(1 - 2\alpha)(m - 2)$ -dimensional received vector at the destination in the noncooperative transmission mode
\mathbf{y}_{d2}	received vector at the destination in the interval when the relay is listening. The dimension is $\alpha(m - 2)$ for AF and repetition DF, and $(1 - \alpha)(m - 2)$ for parallel DF
$\mathbf{y}_{d,r}$	$\alpha(m - 2)$ -dimensional received vector at the destination in the interval when the relay is transmitting
\mathbf{y}_r	received vector at the relay. The dimension is $\alpha(m - 2)$ for AF and repetition DF, and $(1 - \alpha)(m - 2)$ for parallel DF

$$E\{\mathbf{z}_{d2}\mathbf{z}_{d2}^\dagger\} = \sigma_{z_{d2}}^2 \mathbf{I} = \sigma_{\hat{h}_{sd}}^2 E\{\mathbf{x}_{s2}\mathbf{x}_{s2}^\dagger\} + N_0\mathbf{I}, \quad E\{\mathbf{z}_{d,r}\mathbf{z}_{d,r}^\dagger\} = \sigma_{z_{d,r}}^2 \mathbf{I} = \sigma_{\hat{h}_{sd}}^2 E\{\mathbf{x}'_{s2}\mathbf{x}_{s2}^\dagger\} + \sigma_{\hat{h}_{rd}}^2 E\{\mathbf{x}_r\mathbf{x}_r^\dagger\} + N_0\mathbf{I}. \quad (22)$$

Above, \mathbf{x}^\dagger denotes the conjugate transpose of the vector \mathbf{x} . Note that the expressions for the non-overlapped AF scheme can be obtained as a special case of (20)–(22) by setting $\mathbf{x}'_{s2} = 0$.

An achievable rate expression R_{AF} is obtained by solving the following optimization problem which requires finding the worst-case noise:

$$C_{AF} \geq R_{AF} = \inf_{p_{z_{d1}}(\cdot), p_{z_r}(\cdot), p_{z_{d2}}(\cdot), p_{z_{d,r}}(\cdot)} \sup_{p_{x_s}(\cdot)} \frac{1}{m} I(\mathbf{x}_s; \mathbf{y}_d, \mathbf{y}_{d,r} | \hat{h}_{sr}, \hat{h}_{sd}, \hat{h}_{rd}). \quad (23)$$

The following results provides a general formula for R_{AF} , which applies to both non-overlapped and overlapped transmission scenarios.

Theorem 1: An achievable rate for AF transmission scheme is given by

$$R_{AF} = \frac{1}{m} E_{w_{sd}, w_{rd}, w_{sr}} \left\{ (1 - 2\alpha)(m - 2) \log\left(1 + \frac{P_{s1}|\hat{h}_{sd}|^2}{\sigma_{z_{d1}}^2}\right) + (m - 2)\alpha \log\left(1 + \frac{P_{s1}|\hat{h}_{sd}|^2}{\sigma_{z_{d2}}^2}\right) + f\left(\frac{P_{s1}|\hat{h}_{sr}|^2}{\sigma_{z_r}^2}, \frac{P_{r1}|\hat{h}_{rd}|^2}{\sigma_{z_{d,r}}^2}\right) + q\left(\frac{P_{s1}|\hat{h}_{sd}|^2}{\sigma_{z_{d2}}^2}, \frac{P_{s2}|\hat{h}_{sd}|^2}{\sigma_{z_{d,r}}^2}, \frac{P_{s1}|\hat{h}_{sr}|^2}{\sigma_{z_r}^2}, \frac{P_{r1}|\hat{h}_{rd}|^2}{\sigma_{z_{d,r}}^2}\right) \right\} \quad (24)$$

where $f(\cdot)$ and $q(\cdot)$ are defined as $f(x, y) = \frac{xy}{1+x+y}$ and $q(a, b, c, d) = \frac{(1+a)b(1+c)}{1+c+d}$. Furthermore,

$$\frac{P_{s1}|\hat{h}_{sd}|^2}{\sigma_{z_{d1}}^2} = \frac{P_{s1}|\hat{h}_{sd}|^2}{\sigma_{z_{d2}}^2} = \frac{P_{s1}\delta_s m P_s \sigma_{sd}^4}{P_{s1}\sigma_{sd}^2 N_0 + (\sigma_{sd}^2 \delta_s m P_s + N_0)N_0} |w_{sd}|^2 \quad (25)$$

$$\frac{P_{s1}|\hat{h}_{sr}|^2}{\sigma_{z_r}^2} = \frac{P_{s1}\delta_s m P_s \sigma_{sr}^4}{P_{s1}\sigma_{sr}^2 N_0 + (\sigma_{sr}^2 \delta_s m P_s + N_0)N_0} |w_{sr}|^2 \quad (26)$$

$$\frac{P_{r1}|\hat{h}_{rd}|^2}{\sigma_{z_{d,r}}^2} = \frac{P_{r1}\delta_r m P_r \sigma_{rd}^4 (\sigma_{sd}^2 \delta_s m P_s + N_0) |w_{rd}|^2}{P_{s2}\sigma_{sd}^2 N_0 (\sigma_{rd}^2 \delta_r m P_r + N_0) + P_{r1}\sigma_{rd}^2 N_0 (\sigma_{sd}^2 \delta_s m P_s + N_0) + N_0 (\sigma_{sd}^2 \delta_s m P_s + N_0) (\sigma_{rd}^2 \delta_r m P_r + N_0)} \quad (27)$$

$$\frac{P_{s2}|\hat{h}_{sd}|^2}{\sigma_{z_{d,r}}^2} = \frac{P_{s2}\delta_s m P_s \sigma_{sd}^4 (\sigma_{rd}^2 \delta_r m P_r + N_0) |w_{sd}|^2}{P_{s2}\sigma_{sd}^2 N_0 (\sigma_{rd}^2 \delta_r m P_r + N_0) + P_{r1}\sigma_{rd}^2 N_0 (\sigma_{sd}^2 \delta_s m P_s + N_0) + N_0 (\sigma_{sd}^2 \delta_s m P_s + N_0) (\sigma_{rd}^2 \delta_r m P_r + N_0)} \quad (28)$$

In the above equations and henceforth, $w_{sr} \sim \mathcal{CN}(0, 1)$, $w_{sd} \sim \mathcal{CN}(0, 1)$, $w_{rd} \sim \mathcal{CN}(0, 1)$ denote independent, standard Gaussian random variables. The above formulation applies to both overlapped and non-overlapped cases.

Recalling (9), if we assume in (24)–(28) that

$$P_{s1} = \frac{(1 - \delta_s)mP_s}{(m - 2)(1 - \alpha)} \quad \text{and} \quad P_{s2} = 0, \quad (29)$$

we obtain the achievable rate expression for the non-overlapped AF scheme. Note that if $P_{s2} = 0$, the function $q(\cdot, \cdot, \cdot, \cdot) = 0$ in (24). For overlapped AF, we have

$$P_{s1} = P_{s2} = \frac{(1 - \delta_s)mP_s}{m - 2}. \quad (30)$$

Moreover, we know from (10) that

$$P_{r1} = \frac{(1 - \delta_r)mP_r}{(m - 2)\alpha}. \quad (31)$$

Proof: See Appendix A.

Next, we consider DF relaying scheme. In DF, there are two different coding approaches [7], namely repetition coding and parallel channel coding. We first consider repetition channel coding scheme. The following result provides achievable rate expressions for both non-overlapped and overlapped transmission scenarios.

Theorem 2: An achievable rate expression for DF with repetition channel coding transmission scheme is given by

$$R_{DFr} = \frac{(1 - 2\alpha)(m - 2)}{m} E_{w_{sd}} \left\{ \log \left(1 + \frac{P_{s1}|\hat{h}_{sd}|^2}{\sigma_{z_{d1}}^2} \right) \right\} + \frac{(m - 2)\alpha}{m} \min\{I_1, I_2\} \quad (32)$$

where

$$I_1 = E_{w_{sr}} \left\{ \log \left(1 + \frac{P_{s1}|\hat{h}_{sr}|^2}{\sigma_{z_r}^2} \right) \right\}, \quad \text{and} \quad (33)$$

$$I_2 = E_{w_{sd}, w_{rd}} \left\{ \log \left(1 + \frac{P_{s1}|\hat{h}_{sd}|^2}{\sigma_{z_{d2}}^2} + \frac{P_{r1}|\hat{h}_{rd}|^2}{\sigma_{z_{d,r}}^2} + \frac{P_{s2}|\hat{h}_{sd}|^2}{\sigma_{z_{d,r}}^2} + \frac{P_{s1}|\hat{h}_{sd}|^2}{\sigma_{z_{d2}}^2} \frac{P_{s2}|\hat{h}_{sd}|^2}{\sigma_{z_{d,r}}^2} \right) \right\}. \quad (34)$$

$\frac{P_{s1}|\hat{h}_{sd}|^2}{\sigma_{z_{d1}}^2}$, $\frac{P_{s1}|\hat{h}_{sd}|^2}{\sigma_{z_{d2}}^2}$, $\frac{P_{s1}|\hat{h}_{sr}|^2}{\sigma_{z_r}^2}$, $\frac{P_{s2}|\hat{h}_{sd}|^2}{\sigma_{z_{d,r}}^2}$, $\frac{P_{r1}|\hat{h}_{rd}|^2}{\sigma_{z_{d,r}}^2}$ have the same expressions as in (25)–(28). P_{s1} , P_{s2} and P_{r1} are given in (29)–(31).

Proof: See Appendix B.

Finally, we consider DF with parallel channel coding and assume that non-overlapped transmission scheme is

adopted. From [13, Equation (6)], we note that an achievable rate expression is given by

$$\min\{(1 - \alpha)I(\mathbf{x}_s; \mathbf{y}_r | \hat{h}_{sr}), (1 - \alpha)I(\mathbf{x}_s; \mathbf{y}_d | \hat{h}_{sd}) + \alpha I(\mathbf{x}_r; \mathbf{y}_{d,r} | \hat{h}_{rd})\}.$$

Note that we do not have separate direct transmission in this relaying scheme. Using similar methods as in the proofs of Theorems 1 and 2, we obtain the following result. The proof is omitted to avoid repetition.

Theorem 3: An achievable rate of non-overlapped DF with parallel channel coding scheme is given by

$$R_{DFp} = \min \left\{ \frac{(1 - \alpha)(m - 2)}{m} E_{w_{sr}} \left\{ \log \left(1 + \frac{P_{s1} |\hat{h}_{sr}|^2}{\sigma_{z_r}^2} \right) \right\}, \frac{(1 - \alpha)(m - 2)}{m} E_{w_{sd}} \left\{ \log \left(1 + \frac{P_{s1} |\hat{h}_{sd}|^2}{\sigma_{z_{d2}}^2} \right) \right\} \right. \\ \left. + \frac{\alpha(m - 2)}{m} E_{w_{rd}} \left\{ \log \left(1 + \frac{P_{r1} |\hat{h}_{rd}|^2}{\sigma_{z_{d,r}}^2} \right) \right\} \right\} \quad (35)$$

where $\frac{P_{s1} |\hat{h}_{sd}|^2}{\sigma_{z_{d2}}^2}$, $\frac{P_{s1} |\hat{h}_{sr}|^2}{\sigma_{z_r}^2}$, and $\frac{P_{r1} |\hat{h}_{rd}|^2}{\sigma_{z_{d,r}}^2}$ are given in (25)-(27) with P_{s1} and P_{r1} defined in (29) and (31). \square

V. RESOURCE ALLOCATION STRATEGIES

Having obtained achievable rate expressions in Section IV, we now identify resource allocation strategies that maximize these rates. We consider three resource allocation problems: 1) power allocation between training and data symbols; 2) time/bandwidth allocation to the relay; 3) power allocation between the source and relay under a total power constraint.

We first study how much power should be allocated for channel training. In non-overlapped AF, it can be seen that δ_r appears only in $\frac{P_{r1} |\hat{h}_{rd}|^2}{\sigma_{z_{d,r}}^2}$ in the achievable rate expression (24). Since $f(x, y) = \frac{xy}{1+x+y}$ is a monotonically increasing function of y for fixed x , (24) is maximized by maximizing $\frac{P_{r1} |\hat{h}_{rd}|^2}{\sigma_{z_{d,r}}^2}$. We can maximize $\frac{P_{r1} |\hat{h}_{rd}|^2}{\sigma_{z_{d,r}}^2}$ by maximizing the coefficient of the random variable $|w_{rd}|^2$ in (27), and the optimal δ_r is given below:

$$\delta_r^{opt} = \frac{-mP_r\sigma_{rd}^2 - \alpha mN_0 + 2\alpha N_0 + \sqrt{\alpha(m-2)(m^2P_r\sigma_{rd}^2\alpha N_0 + m^2P_r^2\sigma_{rd}^4 + \alpha mN_0^2 + mP_r\sigma_{rd}^2N_0 - 2mP_r\sigma_{rd}^2\alpha N_0 - 2N_0\alpha)}}{mP_r\sigma_{rd}^2(-1 + \alpha m - 2\alpha)}. \quad (36)$$

Optimizing δ_s in non-overlapped AF is more complicated as it is related to all the terms in (24), and hence obtaining an analytical solution is unlikely. A suboptimal solution is to maximize $\frac{P_{s1} |\hat{h}_{sd}|^2}{\sigma_{z_{d1}}^2}$ and $\frac{P_{s1} |\hat{h}_{sr}|^2}{\sigma_{z_r}^2}$ separately, and obtain two solutions $\delta_{s,1}^{subopt}$ and $\delta_{s,2}^{subopt}$, respectively. Note that expressions for $\delta_{s,1}^{subopt}$ and $\delta_{s,2}^{subopt}$ are exactly

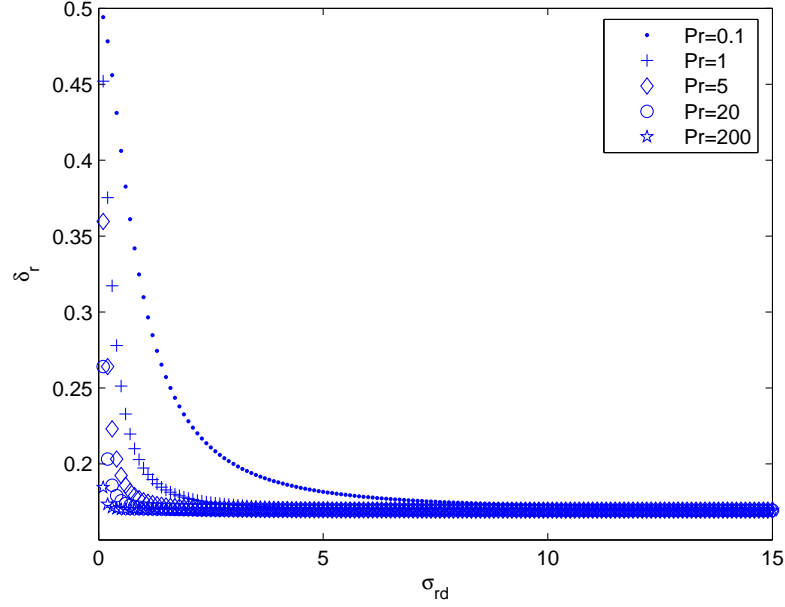


Fig. 4. δ_r vs. σ_{rd} for different values of P_r when $m = 50$.

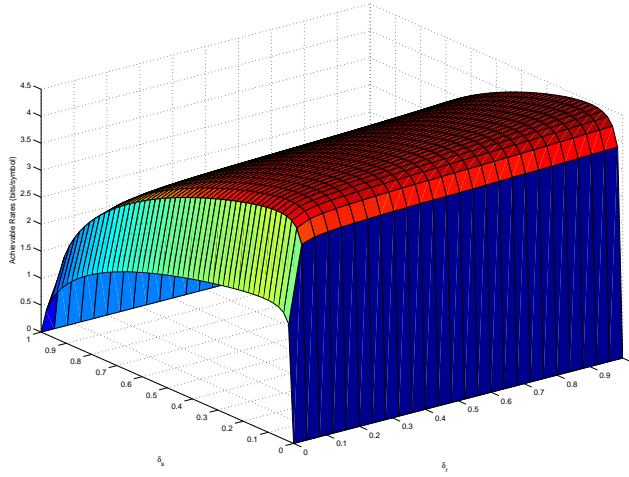


Fig. 5. Overlapped AF achievable rates vs. δ_s and δ_r when $P_s = P_r = 50$

the same as that in (36) with P_r and α replaced by P_s and $(1 - \alpha)$, and σ_{rd} replaced by σ_{sd} in $\delta_{s,1}^{subopt}$ and replaced by σ_{sr} in $\delta_{s,2}^{subopt}$. When the source-relay channel is better than the source-destination channel and the fraction of time over which direct transmission is performed is small, $\frac{P_{s1}|\hat{h}_{sr}|^2}{\sigma_{zr}^2}$ is a more dominant factor and $\delta_{s,2}^{subopt}$ is a good choice for training power allocation. Otherwise, $\delta_{s,1}^{subopt}$ might be preferred. Note that in non-overlapped

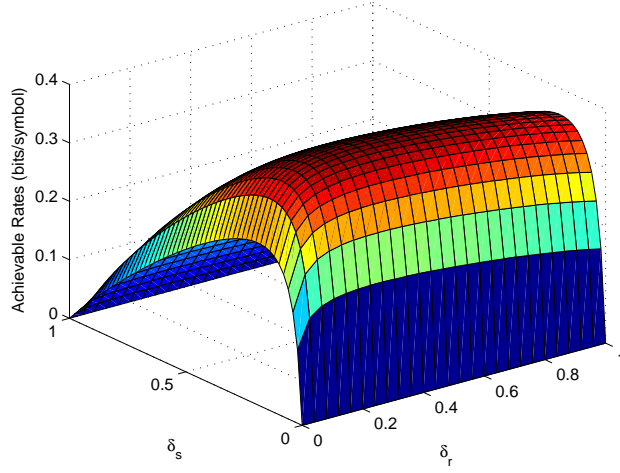


Fig. 6. Overlapped AF achievable rates vs. δ_s and δ_r when $P_s = P_r = 0.5$

DF with repetition and parallel coding, $\frac{P_r |h_{rd}|^2}{\sigma_{z_{d,r}}^2}$ is the only term that includes δ_r . Therefore, similar results and discussions apply. For instance, the optimal δ_r has the same expression as that in (36). Figure 4 plots the optimal δ_r as a function of σ_{rd} for different relay power constraints P_r when $m = 50$ and $\alpha = 0.5$. It is observed in all cases that the allocated training power monotonically decreases with improving channel quality and converges to $\frac{\sqrt{\alpha(m-2)}-1}{\alpha m - 2\alpha - 1} \approx 0.169$ which is independent of P_r .

In overlapped transmission schemes, both δ_s and δ_r appear in more than one term in the achievable rate expressions. Therefore, we resort to numerical results to identify the optimal values. Figures 5 and 6 plot the achievable rates as a function of δ_s and δ_r for overlapped AF. In both figures, we have assumed that $\sigma_{sd} = 1, \sigma_{sr} = 2, \sigma_{rd} = 1$ and $m = 50, N_0 = 1, \alpha = 0.5$. While Fig. 5 considers high SNRs ($P_s = 50$ and $P_r = 50$), we assume that $P_s = 0.5$ and $P_r = 0.5$ in Fig. 6. In Fig. 5, we observe that increasing δ_s will increase achievable rate until $\delta_s \approx 0.1$. Further increase in δ_s decreases the achievable rates. On the other hand, rates always increase with increasing δ_r , leaving less and less power for data transmission by the relay. This indicates that cooperation is not beneficial in terms of achievable rates and direct transmission should be preferred. On the other hand, in the low-power regime considered in Fig. 6, the optimal values of δ_s and δ_r are approximately 0.18 and 0.32, respectively. Hence, the relay in this case helps to improve the rates.

Next, we analyze the effect of the degree of cooperation on the performance in AF and repetition DF. Figures

7 and 8 plot the achievable rates as a function of α which gives the fraction of total time/bandwidth allocated to the relay. Achievable rates are obtained for different channel qualities given by the standard deviations σ_{sd} , σ_{sr} , and σ_{rd} of the fading coefficients. We observe that if the input power is high, α should be either 0.5 or close to zero depending on the channel qualities. On the other hand, $\alpha = 0.5$ always gives us the best performance at low SNR levels regardless of the channel qualities. Hence, while cooperation is beneficial in the low-SNR regime, noncooperative transmissions might be optimal at high SNRs. We note from Fig. 7 in which $P_s = P_r = 50$ that cooperation starts being useful as the source-relay channel variance σ_{sr}^2 increases. Similar results are also observed if overlapped DF with repetition coding is considered. Hence, the source-relay channel quality is one of the key factors in determining the usefulness of cooperation in the high SNR regime. At the same time, additional numerical analysis has indicated that if SNR is further increased, noncooperative direct transmission tends to outperform cooperative schemes even in the case in which $\sigma_{sr} = 10$. Hence, there is a certain relation between the SNR level and the required source-relay channel quality for cooperation to be beneficial. The above conclusions apply to overlapped AF and DF with repetition coding. In contrast, numerical analysis of non-overlapped DF with parallel coding in the high-SNR regime has shown that cooperative transmission with this technique provides improvements over noncooperative direct transmission. A similar result will be discussed later in this section when the performance is analyzed under total power constraints.

In Fig. 8 in which SNR is low ($P_s = P_r = 0.5$), we see that the highest achievable rates are attained when there is full cooperation (i.e., when $\alpha = 0.5$). Note that in this figure, overlapped DF with repetition coding is considered. If overlapped AF is employed as the cooperation strategy, we have similar conclusions but it should also be noted that overlapped AF achieves smaller rates than those attained by overlapped DF with repetition coding.

In Fig. 9, we plot the achievable rates of DF with parallel channel coding, derived in Theorem 3, when $P_s = P_r = 0.5$. We can see from the figure that the highest rate is obtained when both the source-relay and relay-destination channel qualities are higher than that of the source-destination channel (i.e., when $\sigma_{sd} = 1, \sigma_{sr} = 4, \sigma_{rd} = 4$). Additionally, we observe that as the source-relay channel improves, more resources need to be allocated to the relay to achieve the maximum rate. We note that significant improvements with respect to direct transmission (i.e., the case when $\alpha \rightarrow 0$) are obtained. Finally, we can see that when compared to AF and DF with repetition coding,

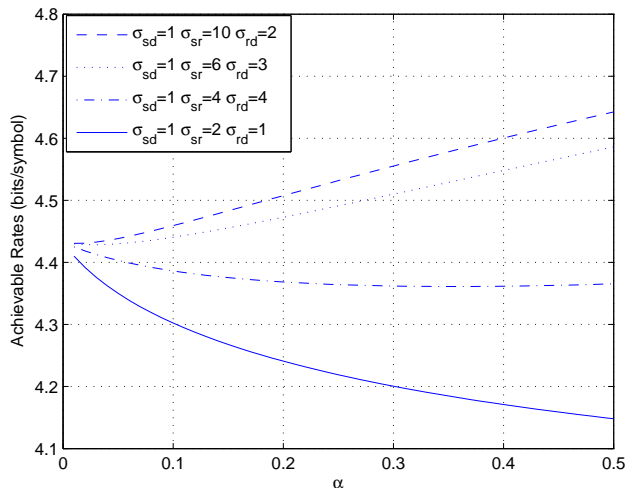


Fig. 7. Overlapped AF achievable rate vs. α when $P_s = P_r = 50$, $\delta_s = \delta_r = 0.1$, $m = 50$.

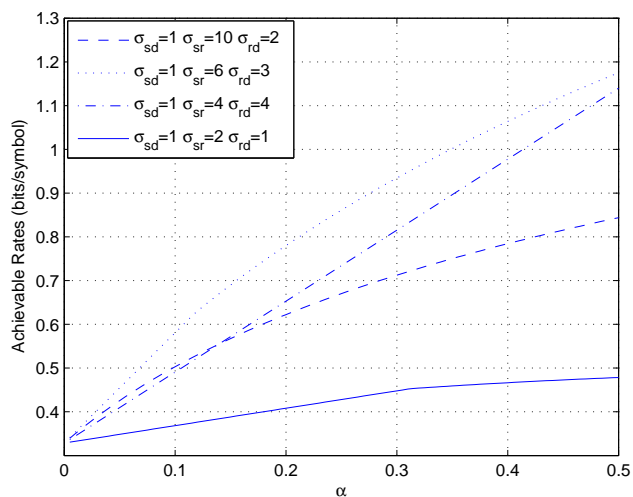


Fig. 8. Overlapped DF with repetition coding achievable rate vs. α when $P_s = P_r = 0.5$, $\delta_s = \delta_r = 0.1$, $m = 50$.

DF with parallel channel coding achieves higher rates. On the other hand, AF and repetition coding DF have advantages in the implementation. Obviously, the relay, which amplifies and forwards, has a simpler task than that which decodes and forwards. Moreover, as pointed out in [18], if AF or repetition coding DF is employed in the system, the architecture of the destination node is simplified because the data arriving from the source and relay can be combined rather than stored separately.

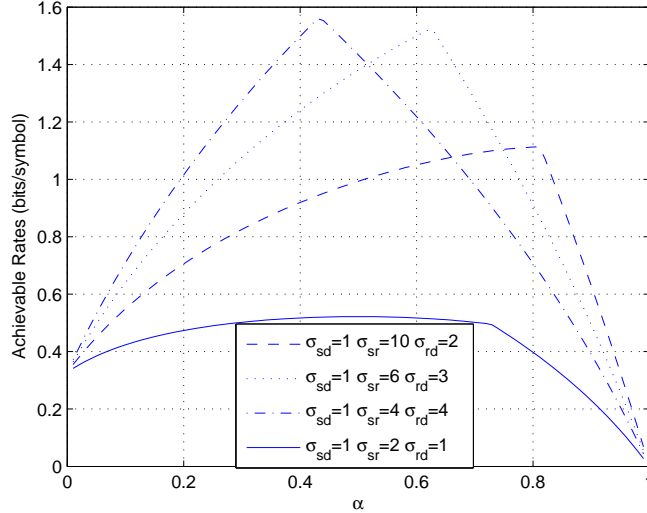


Fig. 9. Non-overlapped DF parallel coding achievable rate vs. α when $P_s = P_r = 0.5$, $\delta_s = \delta_r = 0.1$, $m = 50$.

In certain cases, source and relay are subject to a total power constraint. Here, we introduce the power allocation coefficient θ , and total power constraint P . P_s and P_r have the following relations: $P_s = \theta P$, $P_r = (1 - \theta)P$, and hence $P_s + P_r = P$. Next, we investigate how different values of θ , and hence different power allocation strategies, affect the achievable rates. Analytical results for θ that maximizes the achievable rates are difficult to obtain. Therefore, we again resort to numerical analysis. In all numerical results, we assume that $\alpha = 0.5$ which provides the maximum of degree of cooperation. First, we consider the AF. The fixed parameters we choose are $P = 100$, $N_0 = 1$, $\delta_s = 0.1$, $\delta_r = 0.1$. Fig. 10 plots the achievable rates in the overlapped AF transmission scenario as a function of θ for different channel conditions, i.e., different values of σ_{sr} , σ_{rd} , and σ_{sd} . We observe that the best performance is achieved as $\theta \rightarrow 1$. Hence, even in the overlapped scenario, all the power should be allocated to the source and direct transmission should be preferred at these high SNR levels. Note that if direct transmission is performed, there is no need to learn the relay-destination channel. Since the time allocated to the training for this channel should be allocated to data transmission, the real rate of direct transmission is slightly higher than the point that the cooperative rates converge as $\theta \rightarrow 1$. For this reason, we also provide the direct transmission rate separately in Fig. 10. Further numerical analysis has indicated that direct transmission outperforms non-overlapped AF, overlapped and non-overlapped DF with repetition coding as well at this level of input power. On the other hand, in Fig. 11 which plots the achievable rates of non-overlapped DF with parallel coding as a function of θ ,

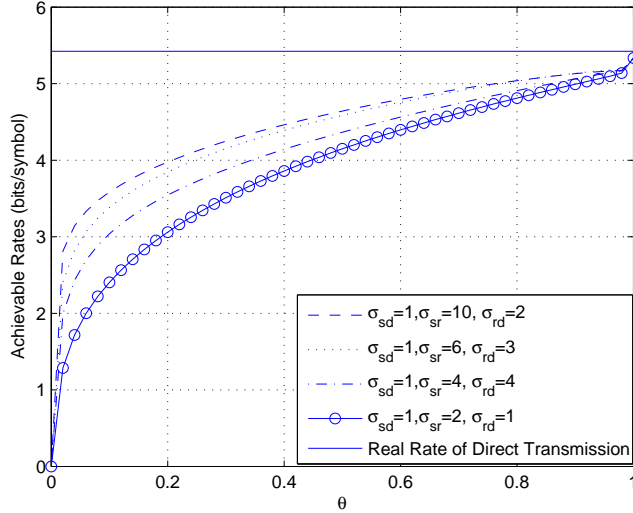


Fig. 10. Overlapped AF achievable rate vs. θ . $P = 100$, $m = 50$.

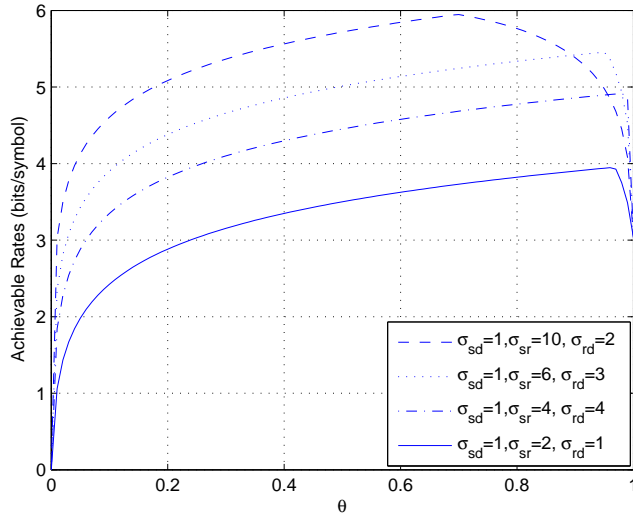


Fig. 11. Non-overlapped Parallel coding DF rate vs. θ . $P = 100$, $m = 50$.

we observe that direct transmission rate, which is the same as that given in Fig. 10, is exceeded if $\sigma_{sr} = 10$ and hence the source-relay channel is very strong. The best performance is achieved when $\theta \approx 0.7$ and therefore 70% of the power is allocated to the source.

Figs. 12 and 13 plot the non-overlapped achievable rates when $P = 1$. In all cases, we observe that performance levels higher than that of direct transmission are achieved unless the qualities of the source-relay and relay-

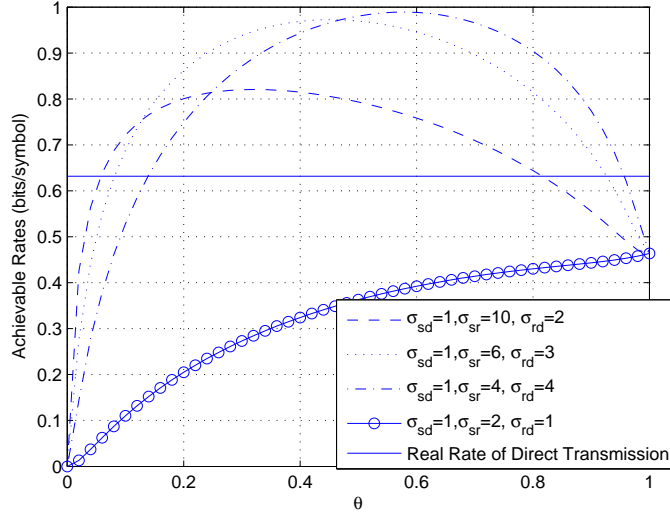


Fig. 12. Non-overlapped AF achievable rate vs. θ . $P = 1$, $m = 50$.

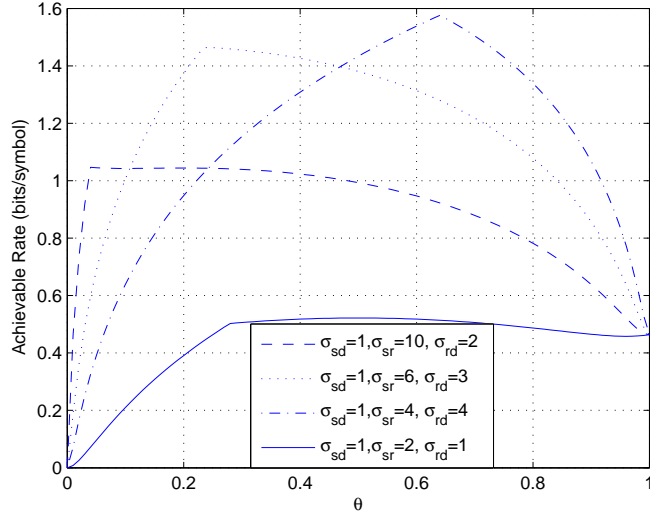


Fig. 13. Non-overlapped Parallel coding DF rate vs. θ . $P = 1$, $m = 50$.

destination channels are comparable to that of the source-destination channel (e.g., $\sigma_{sd} = 1, \sigma_{sr} = 2, \sigma_{rd} = 1$). Moreover, we note that the best performances are attained when the source-relay and relay-destination channels are both considerably better than the source-destination channel (i.e., when $\sigma_{sd} = 1, \sigma_{sr} = 4, \sigma_{rd} = 4$). As expected, highest gains are obtained with parallel coding DF although further numerical analysis has shown that repetition coding incur only small losses. Finally, Fig. 14 plot the achievable rates of overlapped AF when $P = 1$. Similar

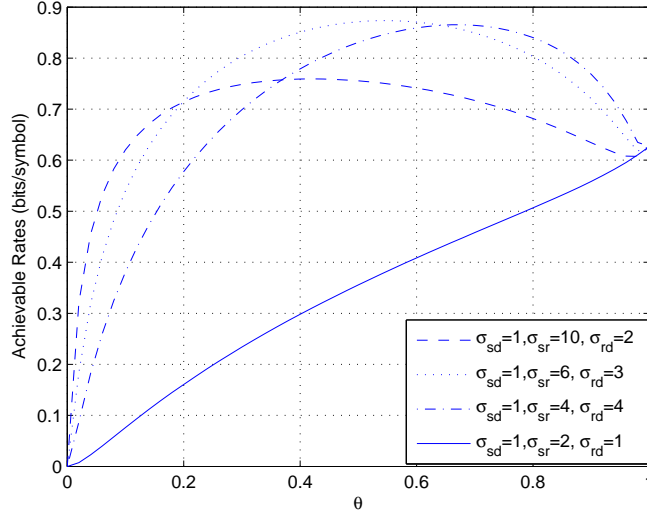


Fig. 14. Overlapped AF achievable rate vs. θ . $P = 1$, $m = 50$.

conclusions apply also here. However, it is interesting to note that overlapped AF rates are smaller than those achieved by non-overlapped AF. This behavior is also observed when DF with repetition coding is considered. Note that in non-overlapped transmission, source transmits in a shorter duration of time with higher power. This signaling scheme provides better performance as expected because it is well-known that flash signaling achieves the capacity in the low-SNR regime in imperfectly known channels [24].

Table II below summarizes the conclusions drawn and insights gained in this section on the performance of different cooperation strategies and resource allocation schemes in the high- and low-SNR regimes.

VI. ENERGY EFFICIENCY

Our analysis has shown that cooperative relaying is generally beneficial in the low-power regime, resulting in higher achievable rates when compared to direct transmission. In this section, we provide an energy efficiency perspective and remark that care should be exercised when operating at very low SNR values. The least amount of energy required to send one information bit reliably is given by² $\frac{E_b}{N_0} = \frac{\text{SNR}}{C(\text{SNR})}$ where $C(\text{SNR})$ is the channel capacity in bits/symbol. In our setting, the capacity will be replaced by the achievable rate expressions and hence the resulting bit energy, denoted by $\frac{E_{b,U}}{N_0}$, provides the least amount of normalized bit energy values in the worst-case

²Note that $\frac{E_b}{N_0}$ is the bit energy normalized by the noise power spectral level N_0 .

TABLE II

<p style="text-align: center;"><i>High-SNR Regime</i></p>	<ul style="list-style-type: none"> • Cooperation employing <i>overlapped AF</i> or <i>DF with repetition coding</i> is beneficial only if the source-relay channel quality is high enough. If this is not the case or SNR is very high, noncooperative direct transmission should be employed. • Cooperation using <i>non-overlapped DF with parallel coding</i> provides improvements over the performance of noncooperative direct transmission, and achieves higher rates than those attained by <i>overlapped AF</i> and <i>DF with repetition coding</i>. • If the system is operating under total power constraints, all the power should be allocated to the source and hence direct transmission should be preferred over <i>overlapped</i> and <i>non-overlapped AF</i>, and <i>overlapped and non-overlapped DF with repetition coding</i>. • Under total power constraints, only <i>non-overlapped DF with parallel coding</i> outperforms noncooperative direct transmission when the source-relay channel is strong.
<p style="text-align: center;"><i>Low-SNR Regime</i></p>	<ul style="list-style-type: none"> • Cooperation is generally beneficial. • The strengths of both the source-relay and relay-destination channels are important factors. • <i>Non-overlapped DF with parallel coding</i> achieves the highest performance levels. In general, non-overlapped transmission methods should be preferred. Also, <i>DF</i> provides higher gains over <i>AF</i>. • Under total power constraints, highest gains over noncooperative direct transmission are attained when both the source-relay and relay-destination channels are considerably stronger than the source-destination channel. • Under total power constraints, noncooperative direct transmission should be preferred if the qualities of both the source-relay and relay-destination channels are comparable to that of the source-destination channel.

scenario and also serves as an upper bound on the achievable bit energy levels in the channel.

We note that in finding the bit energy values, we assume that $\text{SNR} = P/N_0$ where $P = P_r + P_s$ is the total power. The next result provides the asymptotic behavior of the bit energy as SNR decreases to zero.

Theorem 4: The normalized bit energy in all relaying schemes grows without bound as the signal-to-noise ratio

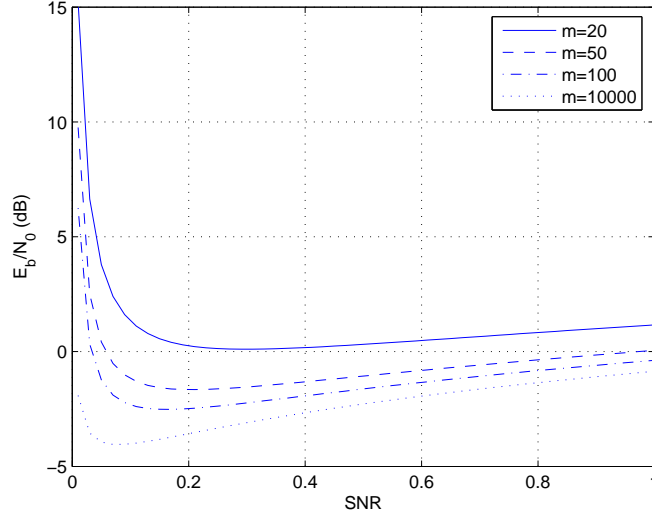


Fig. 15. Non-overlapped AF $E_{b,U}/N_0$ vs. SNR

decreases to zero, i.e.,

$$\left. \frac{E_{b,U}}{N_0} \right|_{R=0} = \lim_{\text{SNR} \rightarrow 0} \frac{\text{SNR}}{R(\text{SNR})} = \frac{1}{\dot{R}(0)} = \infty. \quad (37)$$

Proof: $\dot{R}(0)$ is the derivative of R with respect to SNR as $\text{SNR} \rightarrow 0$. The key point to prove this theorem is to show that when $\text{SNR} \rightarrow 0$, the mutual information decreases as SNR^2 , and hence $\dot{R}(0) = 0$. This can be easily shown because when $P \rightarrow 0$, in all the terms, $\frac{P_{s1}|\hat{h}_{sd}|^2}{\sigma_{z_{d1}}^2}$, $\frac{P_{s1}|\hat{h}_{sd}|^2}{\sigma_{z_{d2}}^2}$, $\frac{P_{s1}|\hat{h}_{sr}|^2}{\sigma_{z_r}^2}$, $\frac{P_{s2}|\hat{h}_{sd}|^2}{\sigma_{z_{d,r}}^2}$ and $\frac{P_{r1}|\hat{h}_{rd}|^2}{\sigma_{z_{d,r}}^2}$ in Theorems 1-3, the denominator goes to a constant while the numerator decreases as P^2 . Hence, these terms diminish as SNR^2 . Since $\log(1+x) = x + o(x)$ for small x , where $o(x)$ satisfies $\lim_{x \rightarrow 0} \frac{o(x)}{x} = 0$, we conclude that the achievable rate expressions also decrease as SNR^2 as SNR vanishes. \square

Theorem 4 indicates that it is extremely energy-inefficient to operate at very low SNR values. We identify the most energy-efficient operating points in numerical results. We choose the following numerical values for the fixed parameters: $\delta_s = \delta_r = 0.1$, $\sigma_{sd} = 1$, $\sigma_{sr} = 4$, $\sigma_{rd} = 4$, $\alpha = 0.5$, and $\theta = 0.6$. Fig. 15 plots the bit energy curves as a function of SNR for different values of m in the non-overlapped AF case. We can see from the figure that the minimum bit energy, which is achieved at a nonzero value of SNR, decreases with increasing m and is achieved at a lower SNR value. Fig. 16 shows the minimum bit energy for different relaying schemes with overlapped or non-overlapped transmission techniques. We observe that the minimum bit energy decreases with increasing m in

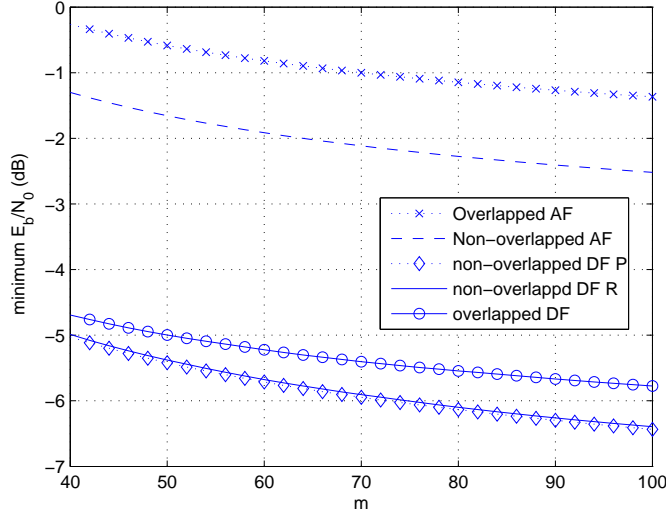


Fig. 16. $E_{b,U}/N_0$ vs. m for different transmission scheme

all cases. We realize that DF is in general much more energy-efficient than AF. Moreover, we note that employing non-overlapped rather than overlapped transmission improves the energy efficiency. We further remark that the performances of non-overlapped DF with repetition coding and parallel coding are very close.

VII. CONCLUSION

In this paper, we have studied the imperfectly-known fading relay channels. We have assumed that the source-destination, source-relay, and relay-destination channels are not known by the corresponding receivers a priori, and transmission starts with the training phase in which the channel fading coefficients are learned with the assistance of pilot symbols, albeit imperfectly. Hence, in this setting, relaying increases the channel uncertainty in the system, and there is increased estimation cost associated with cooperation. We have investigated the performance of relaying by obtaining achievable rates for AF and DF relaying schemes. We have considered both non-overlapped and overlapped transmission scenarios. We have controlled the degree of cooperation by varying the parameter α . We have identified resource allocation strategies that maximize the achievable rate expressions. We have observed that if the source-relay channel quality is low, then cooperation is not beneficial and direct transmission should be preferred at high SNRs when amplify-and-forward or decode-and-forward with repetition coding is employed as the cooperation strategy. On the other hand, we have seen that relaying generally improves the performance

at low SNRs. We have noted that DF with parallel coding provides the highest rates. Additionally, under total power constraints, we have studied power allocation between the source and relay. We have again pointed out that relaying degrades the performance at high SNRs unless DF with parallel channel coding is used and the source-relay channel quality is high. The benefits of relaying is again demonstrated at low SNRs. We have noted that non-overlapped transmission is superior compared to overlapped one in this regime. Finally, we have considered the energy efficiency in the low-power regime, and proved that the bit energy increases without bound as SNR diminishes. Hence, operation at very low SNR levels should be avoided. From the energy efficiency perspective, we have again observed that non-overlapped transmission provides better performance. We have also noted that DF is more energy efficient than AF.

APPENDIX

A. Proof of Theorem 1

Note that in AF relaying,

$$I(\mathbf{x}_s; \mathbf{y}_d, \mathbf{y}_{d,r} | \hat{h}_{sr}, \hat{h}_{sd}, \hat{h}_{rd}) = I(\mathbf{x}_{s1}; \mathbf{y}_{d1} | \hat{h}_{sd}) + I(\mathbf{x}_{s2}; \mathbf{y}_{d2}, \mathbf{y}_{d,r} | \hat{h}_{sr}, \hat{h}_{sd}, \hat{h}_{rd}) \quad (38)$$

where the first mutual expression on the right-hand side of (38) is for the direct transmission and the second is for the cooperative transmission. In the direct transmission, we have

$$\mathbf{y}_{d1} = \hat{h}_{sd} \mathbf{x}_{s1} + \mathbf{z}_{d1}. \quad (39)$$

In this setting, it is well-known that the worst-case noise \mathbf{z}_{d1} is Gaussian [26, Appendix] and \mathbf{x}_{s1} with independent Gaussian components achieves

$$\inf_{p_{z_{d1}}(\cdot)} \sup_{p_{x_{s1}}(\cdot)} I(\mathbf{x}_{s1}; \mathbf{y}_{d1} | \hat{h}_{sd}) = E \left\{ (1 - 2\alpha)(m - 2) \log \left(1 + \frac{P'_{s1} |\hat{h}_{sd}|^2}{\sigma_{z_{d1}}^2} \right) \right\}. \quad (40)$$

We now investigate the cooperative phase. Comparing (14) and (15) with (17) and (18), we see that non-overlapped can be obtained as a special case of overlapped AF scheme by letting $x'_{s2} = 0$. Therefore, we concentrate on the more general case of overlapped transmission. For better illustration, we rewrite the symbol-wise channel input-

output relationships in the following:

$$y_r[i] = \hat{h}_{sr}x_{s2}[i] + z_r[i], \quad y_{d2}[i] = \hat{h}_{sd}x_{s2}[i] + z_{d2}[i], \quad (41)$$

for $i = 1 + (1 - 2\alpha)(m - 2), \dots, (1 - \alpha)(m - 2)$, and

$$y_{d,r}[i] = \hat{h}_{sd}x'_{s2}[i] + \hat{h}_{rd}x_r[i] + z_{d,r}[i], \quad (42)$$

for $i = (1 - \alpha)(m - 2) + 1, \dots, m - 2$. In AF, the signals received and transmitted by the relay have following relation:

$$x_r[i] = \beta y_r[i - \alpha(m - 2)], \quad \text{where} \quad \beta \leq \sqrt{\frac{E\{|x_r|^2\}}{|\hat{h}_{sr}|^2 E\{|x_{s2}|^2\} + E\{|z_r|^2\}}}. \quad (43)$$

Now, we can write the channel in the vector form

$$\underbrace{\begin{pmatrix} y_{d2}[i] \\ y_{d,r}[i + \alpha(m - 2)] \end{pmatrix}}_{\check{\mathbf{y}}_d[i]} = \underbrace{\begin{pmatrix} \hat{h}_{sd} & 0 \\ \hat{h}_{rd}\beta\hat{h}_{sr} & \hat{h}_{sd} \end{pmatrix}}_A \underbrace{\begin{pmatrix} x_s[i] \\ x_s[i + \alpha(m - 2)] \end{pmatrix}}_{\check{\mathbf{x}}_s[i]} + \underbrace{\begin{pmatrix} 0 & 1 & 0 \\ \hat{h}_{rd}\beta & 0 & 1 \end{pmatrix}}_B \underbrace{\begin{pmatrix} z_r[i] \\ z_{d2}[i] \\ z_{d,r}[i + \alpha(m - 2)] \end{pmatrix}}_{\mathbf{z}[i]} \quad (44)$$

where $i = 1 + (1 - 2\alpha)(m - 2), \dots, (1 - \alpha)(m - 2)$ and $\beta \leq \sqrt{\frac{E\{|x_r|^2\}}{|\hat{h}_{sr}|^2 E\{|x_s|^2\} + E\{|z_r|^2\}}}$. Note that we have defined $\mathbf{x}_s = [\mathbf{x}_{s1}^T, \mathbf{x}_{s2}^T, \mathbf{x}_{s2}^T]^T$, and the expression in (44) uses the property that $x_{s2}(j) = x_s(j + (1 - 2\alpha)(m - 2))$ and $x'_{s2}(j) = x_s(j + (1 - \alpha)(m - 2))$ for $j = 1, \dots, \alpha(m - 2)$. The input-output mutual information in the cooperative phase can now be expressed as

$$I(\mathbf{x}_{s2}, \mathbf{x}'_{s2}; \mathbf{y}_{d2}, \mathbf{y}_{d,r} | \hat{h}_{sr}, \hat{h}_{sd}, \hat{h}_{rd}) = \sum_{i=1+(1-2\alpha)(m-2)}^{(1-\alpha)(m-2)} I(\check{\mathbf{x}}_s[i]; \check{\mathbf{y}}_d[i] | \hat{h}_{sr}, \hat{h}_{sd}, \hat{h}_{rd}) = \alpha(m - 2) I(\check{\mathbf{x}}_s; \check{\mathbf{y}}_d | \hat{h}_{sr}, \hat{h}_{sd}, \hat{h}_{rd}) \quad (45)$$

where in (45) we removed the dependence on i without loss of generality. Note that $\check{\mathbf{x}}_s$ and $\check{\mathbf{y}}_d$ are defined in (44).

Now, we can calculate the worst-case capacity by proving that Gaussian distribution for z_r , z_{d2} , and $z_{d,r}$ provides the worst case. We employ techniques similar to that in [26, Appendix]. Any set of particular distributions for z_r , z_{d2} , and $z_{d,r}$ yields an upper bound on the worst case. Let us choose z_r , z_{d2} , and $z_{d,r}$ to be zero mean complex

Gaussian distributed. Then as in [6, Appendix II],

$$\inf_{p_{z_r}(\cdot), p_{z_{d2}}(\cdot), p_{z_{d,r}}(\cdot)} \sup_{p_{x_{s2}}(\cdot), p_{x'_{s2}}(\cdot)} I(\tilde{\mathbf{x}}_s; \tilde{\mathbf{y}}_d | \hat{h}_{sr}, \hat{h}_{sd}, \hat{h}_{rd}) \leq E \log \det \left(\mathbf{I} + (AE\{\tilde{\mathbf{x}}_s \tilde{\mathbf{x}}_s^\dagger\} A^\dagger)(BE\{\mathbf{z}\mathbf{z}^\dagger\} B^\dagger)^{-1} \right) \quad (46)$$

where the expectation is with respect to the fading estimates. To obtain a lower bound, we compute the mutual information for the channel in (44) assuming that \tilde{x}_s is a zero-mean complex Gaussian with variance $E\{\tilde{\mathbf{x}}_s \tilde{\mathbf{x}}_s^\dagger\}$, but the distributions of noise components z_r , z_{d2} , and $z_{d,r}$ are arbitrary. In this case, we have

$$\begin{aligned} I(\tilde{\mathbf{x}}_s; \tilde{\mathbf{y}}_d | \hat{h}_{sr}, \hat{h}_{sd}, \hat{h}_{rd}) &= h(\tilde{\mathbf{x}}_s | \hat{h}_{sr}, \hat{h}_{sd}, \hat{h}_{rd}) - h(\tilde{\mathbf{x}}_s | \tilde{\mathbf{y}}_d, \hat{h}_{sr}, \hat{h}_{sd}, \hat{h}_{rd}) \\ &\geq \log \pi e E\{\tilde{\mathbf{x}}_s \tilde{\mathbf{x}}_s^\dagger\} - \log \pi e \text{var}(\tilde{\mathbf{x}}_s | \tilde{\mathbf{y}}_d, \hat{h}_{sr}, \hat{h}_{sd}, \hat{h}_{rd}) \end{aligned} \quad (47)$$

where the inequality is due to the fact that Gaussian distribution provides the largest entropy and hence [32, Chap. 9]

$$h(\tilde{\mathbf{x}}_s | \tilde{\mathbf{y}}_d, \hat{h}_{sr}, \hat{h}_{sd}, \hat{h}_{rd}) \leq \log \pi e \text{var}(\tilde{\mathbf{x}}_s | \tilde{\mathbf{y}}_d, \hat{h}_{sr}, \hat{h}_{sd}, \hat{h}_{rd}).$$

Above, $h(\cdot)$ denotes the differential entropy functional. From [26, Lemma 1, Appendix], we know that

$$\text{var}(\tilde{\mathbf{x}}_s | \tilde{\mathbf{y}}_d, \hat{h}_{sr}, \hat{h}_{sd}, \hat{h}_{rd}) \leq E \left\{ (\tilde{\mathbf{x}}_s - \hat{\tilde{\mathbf{x}}}_s)(\tilde{\mathbf{x}}_s - \hat{\tilde{\mathbf{x}}}_s)^\dagger | \hat{h}_{sr}, \hat{h}_{sd}, \hat{h}_{rd} \right\} \quad (48)$$

for any estimate $\hat{\tilde{\mathbf{x}}}_s$ given $\tilde{\mathbf{y}}_d, \hat{h}_{sr}, \hat{h}_{sd},$ and \hat{h}_{rd} . If we substitute the linear minimum mean-square-error (LMMSE) estimate $\hat{\tilde{\mathbf{x}}}_s = R_{\tilde{\mathbf{x}}\tilde{\mathbf{y}}} R_{\tilde{\mathbf{y}}}^{-1} \tilde{\mathbf{y}}_d$, where $R_{\tilde{\mathbf{x}}\tilde{\mathbf{y}}}$ and $R_{\tilde{\mathbf{y}}}$ are cross-covariance and covariance matrices respectively, into (47) and (48), we obtain³

$$I(\tilde{\mathbf{x}}_s; \tilde{\mathbf{y}}_d | \hat{h}_{sr}, \hat{h}_{sd}, \hat{h}_{rd}) \geq E \log \det \left(\mathbf{I} + (E\{|x_s|^2\} A A^\dagger)(B E\{\mathbf{z}\mathbf{z}^\dagger\} B^\dagger)^{-1} \right). \quad (49)$$

Since the lower bound (49) applies for any noise distribution, we can easily see that

$$\inf_{p_{z_r}(\cdot), p_{z_{d2}}(\cdot), p_{z_{d,r}}(\cdot)} \sup_{p_{x_{s2}}(\cdot), p_{x'_{s2}}(\cdot)} I(x_s; \tilde{\mathbf{y}}_d | \hat{h}_{sr}, \hat{h}_{sd}, \hat{h}_{rd}) \geq E \log \det \left(\mathbf{I} + (AE\{\tilde{\mathbf{x}}_s \tilde{\mathbf{x}}_s^\dagger\} A^\dagger)(BE\{\mathbf{z}\mathbf{z}^\dagger\} B^\dagger)^{-1} \right). \quad (50)$$

³Here, we use the property that $\det(\mathbf{I} + \mathbf{A}\mathbf{B}) = \det(\mathbf{I} + \mathbf{B}\mathbf{A})$.

From (46) and (50), we conclude that

$$\begin{aligned}
\inf_{p_{z_r}(\cdot), p_{z_{d2}}(\cdot), p_{z_{d,r}}(\cdot)} \sup_{p_{x_{s2}}(\cdot), p_{x'_{s2}}(\cdot)} I(x_s; \check{\mathbf{y}}_d | \hat{h}_{sr}, \hat{h}_{sd}, \hat{h}_{rd}) &= E \log \det \left(\mathbf{I} + (AE\{\check{\mathbf{x}}_s \check{\mathbf{x}}_s^\dagger\}A^\dagger)(BE\{\mathbf{z}\mathbf{z}^\dagger\}B^\dagger)^{-1} \right) \quad (51) \\
&= E \log \left\{ 1 + \frac{P_{s1}|\hat{h}_{sd}|^2}{\sigma_{z_{d2}}^2} + f\left(\frac{P_{s1}|\hat{h}_{sr}|^2}{\sigma_{z_r}^2}, \frac{P_{r1}|\hat{h}_{rd}|^2}{\sigma_{z_{d,r}}^2}\right) \right. \\
&\quad \left. + q\left(\frac{P_{s1}|\hat{h}_{sd}|^2}{\sigma_{z_{d2}}^2}, \frac{P_{s2}|\hat{h}_{sd}|^2}{\sigma_{z_{d,r}}^2}, \frac{P_{s1}|\hat{h}_{sr}|^2}{\sigma_{z_r}^2}, \frac{P_{r1}|\hat{h}_{rd}|^2}{\sigma_{z_{d,r}}^2}\right) \right\} \quad (52)
\end{aligned}$$

In obtaining (52), we have used the fact that $E\{\check{\mathbf{x}}_s \check{\mathbf{x}}_s^\dagger\} = \begin{pmatrix} P_{s1} & 0 \\ 0 & P_{s2} \end{pmatrix}$. Note also that in (52), P_{s1} , P_{s2} and P_{r1} are the powers of source and relay symbols and are given in (29)–(31). Moreover, $\sigma_{z_{d2}}^2$, $\sigma_{z_r}^2$, $\sigma_{z_{d,r}}^2$ are the variances of the noise components defined in (20). Now, combining (23), (38), (40), and (52), we obtain the achievable rate expression in (24). Note that (25)–(28) are obtained by using the expressions for the channel estimates in (5)–(7) and noise variances in (21) and (22). \square

B. Proof of Theorem 2

For DF with repetition coding in overlapped transmission, an achievable rate expression is

$$I(\mathbf{x}_{s1}; \mathbf{y}_{d1} | \hat{h}_{sd}) + \min \left\{ I(\mathbf{x}_{s2}; \mathbf{y}_r | \hat{h}_{sr}), I(\mathbf{x}_{s2}, \mathbf{x}'_{s2}; \mathbf{y}_d, \mathbf{y}_{d,r} | \hat{h}_{sd}, \hat{h}_{rd}) \right\}. \quad (53)$$

Note that the first and second mutual information expressions in (53) are for the direct transmission between the source and destination, and direct transmission between the source and relay, respectively. Therefore, as in the proof of Theorem 1, the worst-case achievable rates can be immediately seen to be equal to the first term on the right-hand side of (32) and I_1 , respectively.

In repetition coding, after successfully decoding the source information, the relay transmits the same codeword as the source. As a result, the input-output relation in the cooperative phase can be expressed as

$$\underbrace{\begin{pmatrix} y_{d2}[i] \\ y_{d,r}[i + \alpha(m-2)] \end{pmatrix}}_{\check{\mathbf{y}}_d[i]} = \underbrace{\begin{pmatrix} \hat{h}_{sd} & 0 \\ \hat{h}_{rd}\beta & \hat{h}_{sd} \end{pmatrix}}_A \underbrace{\begin{pmatrix} x_s[i] \\ x_s[i + \alpha(m-2)] \end{pmatrix}}_{\check{\mathbf{x}}_s[i]} + \underbrace{\begin{pmatrix} z_{d2}[i] \\ z_{d,r}[i + \alpha(m-2)] \end{pmatrix}}_{\mathbf{z}[i]}. \quad (54)$$

where $\beta \leq \sqrt{\frac{E\{|x_r|^2\}}{E\{|x_s|^2\}}}$. From (54), it is clear that the knowledge of \hat{h}_{sr} is not required at the destination. We can easily see that (54) is a simpler expression than (44) in the AF case, therefore we can adopt the same methods as employed in the proof of Theorem 1 to show that Gaussian noise is the worst noise and I_2 is the worst-case rate.

□

REFERENCES

- [1] E. C. van der Meulen, "Three-terminal communication channels," *Adv. Appl. Probab.*, vol. 3, pp. 120-154, 1971.
- [2] T. M. Cover and A.A. El Gamal, "Capacity theorems for the relay channel," *IEEE Trans. Inf. Theory*, vol. IT-25, no. 5, pp. 572-584, Sep. 1979.
- [3] A. A. El Gamal and M. Aref, "The capacity of the semideterministic relay channel," *IEEE Trans. Inf. Theory*, vol. IT-28, no. 3, pp. 536-536, May 1982.
- [4] A. Sendonaris, E. Erkip, and B. Aazhang, "User cooperation diversity-Part I: System description," *IEEE Trans. Commun.*, vol. 51, no. 11, pp. 1927-1938, Nov. 2003.
- [5] A. Sendonaris, E. Erkip, and B. Aazhang, "User cooperation diversity-Part II: Implementation aspects and performance analysis," *IEEE Trans. Commun.*, vol. 51, no. 11, pp. 1939-1948, Nov. 2003.
- [6] J.N. Laneman, D.N.C. Tse, G.W. Wornel "Cooperative diversity in wireless networks: Efficient protocols and outage behavior," *IEEE Trans. Inform. Theory*, vol.50,pp.3062-3080. Dec.2004
- [7] J. N. Laneman, "Cooperation in wireless networks: Principles and applications," Springer, 2006, ch.1 Cooperative Diversity: Models, Algorithms, and Architectures
- [8] R.U. Nabar, H. Bolcskei, F.W. Kneubuhler, "Fading Relay Channels:Performance Limits and Space-Time Signal Design," *IEEE J.Select. Areas Commun.* vol.22,NO.6 pp. 1099-1109. Aug.2004
- [9] A. Host-Madsen and J. Zhang, "Capacity bounds and power allocation for wireless relay channels," *IEEE Trans. Inform. Theory*, vol. 51, no. 6, pp. 2020-2040, June. 2005.
- [10] D. Gunduz and E. Erkip, "Opportunistic cooperation by dynamic resource allocation," *IEEE Trans. Wireless. Commun.*, vol. 6, no. 4, pp. 1446-1454, Apr. 2007.
- [11] Y. Yao, X. Cai, and G. B. Giannakis, "On energy efficiency and optimum resource allocation of relay transmissions in the low-power regime," *IEEE Trans. Wireless Commun.*, vol. 4, no. 6, pp. 2917-2927, Nov. 2005.
- [12] Y. Liang, V. V. Veeravalli, and H. Vincent Poor, "Resource allocation for wireless fading relay channels: Max-Min solution," *IEEE Trans. Inform. Theory*, vol. 53, no. 10, pp. 3432-3453, Oct. 2007.
- [13] Y. Liang and V. V. Veeravalli, "Gaussian orthogonal relay channels: Optimal resource allocation and capacity," *IEEE Trans. Inform. Theory*, vol. 51, no. 9, pp. 3284-3289, Sept. 2005.
- [14] C.T.K.Ng and A.Goldsmith, "The impact of CSI and power allocation on relay channel capacity and cooperation strategies," *IEEE Trans. Wireless Commun.*, vol. 7, no. 12, pp. 5380-5389, Dec. 2008.
- [15] A. Host-Madsen, "Capacity bounds for cooperative diversity," *IEEE Trans. Inform. Theory*, vol. 52, no. 4, pp. 1522-1544, Apr. 2006.
- [16] G. Kramer, M. Gastpar, and P. Gupta, "Cooperative strategies and capacity theorems for relay networks," *IEEE Trans. Inform. Theory*, vol. 51, no. 9, pp. 3037-3063, Sept. 2005.
- [17] P. Mitran, H. Ochiai, and V. Tarokh, "Space-time diversity enhancements using collaborative communications," *IEEE Trans. Inform. Theory*, vol. 51, no. 6, pp. 2041-2057, June 2005.

- [18] G. Kramer, I. Marić, and R. D. Yates, "Cooperative communications," *Foundations and Trends in Networking*. Hanover, MA: NOW Publishers Inc., vol. 1, no. 3-4, pp. 271-425, 2006.
- [19] Special Issue on Models, Theory, and Codes for Relaying and Cooperation in Communication Networks, *IEEE Tran. Inform. Theory*, vol.53, no.9, Oct. 2007.
- [20] B. Wang, J. Zhang, and L. Zheng, "Achievable rates and scaling laws of power-constrained wireless sensory relay networks" *IEEE Tran. Inform. Theory*, vol.52, no.9, Sep.2006.
- [21] F. Gao, T. Cui, and A. Nallanathan, "On channel estimation and optimal training design for amplify and forward relay networks" *IEEE Trans. Wireless. Commun.*, vol.7, no.5 part 2 pp.1907 - 1916, 2008
- [22] C. S. Patel and G. L. Stüber "Channel estimation for amplify and forward relay based cooperation diversity systems," *IEEE Trans. Wireless. Comm*, vol.6, no.6 pp. 2348-2356, 2007.
- [23] A.S. Avestimehr and D.N.C. Tse, "Outage capacity of the fading relay channel in the low-SNR regime," *IEEE Trans. Inform. Theory*, vol.53, pp.1401 - 1415, April 2007.
- [24] S. Verdú, "Spectral efficiency in the wideband regime," *IEEE Trans. Inform. Theory*, vol. 48, pp. 1319-1343, June 2002.
- [25] M. Medard "The effect upon channel capacity in wireless communication of perfect and imperfect knowledge of the channel," *IEEE Trans. Inform. Theory*, vol.46,pp.933-946,May.2000
- [26] B. Hassibi and B. M. Hochwald, "How much training is needed in multiple-antenna wireless link?,"*IEEE Trans. Inform. Theory*, vol.49,pp.951-964,April 2003
- [27] L. Tong, B. M. Sadler, and M. Dong, "Pilot-assisted wireless transmission," *IEEE Signal Processing Mag.*, pp. 12-25, Nov. 2004.
- [28] J. Zhang and M.C. Gursoy, "To cooperate, or not to cooperate in imperfectly known fading channels," Proc.of the 9th IEEE International Workshop on Signal Processing Advances in Wireless Communications (SPAWC), 2008.
- [29] S. Akin and M.C. Gursoy, "Achievable rates and training optimization for fading relay channels with memory," Proc. of the 42nd Annual Conference on Information Sciences and Systems (CISS), Princeton University, 2008.
- [30] J. Zhang and M.C. Gursoy, "Achievable rates and optimal resource allocation for imperfectly-known relay channels," Proc. of the 45th Annual Allerton Conference on Communication, Control and Computing, University of Illinois at Urbana-Champaign, Sept. 2007.
- [31] M.C. Gursoy, "An energy efficiency perspective on training for fading channels," Proceedings of the IEEE ISIT 2007.
- [32] T. M. Cover and J. A. Thomas, *Elements of Information Theory*. New York: Wiley, 1991.